Available online at www.sciencedirect.com

ScienceDirect

Energy Procedia 101 (2016) 1240 – 1247

Energy Procedia

71st Conference of the Italian Thermal Machines Engineering Association, ATI2016, 14-16 September 2016, Turin, Italy

Modeling and experimental activities on a small-scale sliding vane pump for ORC-based waste heat recovery applications

Giuseppe Bianchi[a,b]*, Fabio Fatigati[a], Stefano Murgia[c], Roberto Cipollone[a], Giulio Contaldi[c]

[a]*University of L'Aquila, via Giovanni Gronchi 18, L'Aquila 67100, Italy*
[b]*Brunel University London, Kingston Lane, Uxbridge UB8 3PH, United Kingdom*
[c]*Ing. Enea Mattei S.p.A.,Strada Padana Superiore 307, Vimodrone 20090, Italy*

Abstract

Pumping work in energy recovery units based on Organic Rankine Cycles (ORC) can severely affect the net power output recovered. Nevertheless, in recent years scientific and industrial communities mainly focused on expanders' development. In order to address this lack of know-how and equipment, the current paper presents the development of a positive displacement ORC pump based on the sliding vane rotary technology. The machine was installed in a power unit for low-medium grade thermal energy recovery that operated with oil at 70-120°C as upper thermal source and tap water as lower one. Working fluid was R236fa while cycle pressure ratio ranged from 2.8 to 3.7. The ORC pump was also tested at different revolution speeds such that mass flow rate varied between 0.05 kg/s and 0.12 kg/s. These experimental data were further used to validate a comprehensive one-dimensional model that takes into account fluid dynamic filling and emptying processes, closed vane transformation and leakages at blade tip, rotor slots and end walls clearances. Viscous and dry friction phenomena occurring between components in relative motion were additionally considered. A full operating map of the sliding vane pump was eventually retrieved to explore multiple off-design operating conditions. The parametric and modular structure of the model will act as a design platform to outline enhanced ORC sliding vane pump prototypes.

© 2016 The Authors. Published by Elsevier Ltd. This is an open access article under the CC BY-NC-ND license (http://creativecommons.org/licenses/by-nc-nd/4.0/).

Peer-review under responsibility of the Scientific Committee of ATI 2016.

Keywords: sliding vane pump; positive displacement pump; ORC; waste heat recovery; GT-SUITE

* Corresponding author. Tel.: +44 (0)1895 267707
E-mail address: giuseppe.bianchi@brunel.ac.uk

1876-6102 © 2016 The Authors. Published by Elsevier Ltd. This is an open access article under the CC BY-NC-ND license (http://creativecommons.org/licenses/by-nc-nd/4.0/).
Peer-review under responsibility of the Scientific Committee of ATI 2016.
doi:10.1016/j.egypro.2016.11.139

Nomenclature

A	surface area [m^2]	f_{dry}	dry friction coefficient
D_{eq}	equivalent diameter [m]	$\dot{m}$	mass flow rate [kg/s]
F_N	normal force [N]	Δp	pressure rise [Pa]
F_{FD}	dry friction force [N]	t	time [s]
F_{FV}	viscous friction force [N]	η	efficiency
L	cell axial length [m]	μ	dynamic viscosity [Pa·s]
N	number of cells	ρ	density [kg/m^3]
T	torque [Nm]	ω	revolution speed [rad/s]
V	cell volume [m^3]	du/dy	velocity gradient along the clearance [m^{-1}]

1. Introduction

Growing awareness in environmental concerns currently demands greater efforts towards solutions that, in the energy sector, mean renewable sources, recovery and saving. All these areas of intervention are indeed effectively able to impact against the carbon accumulation in the atmosphere, the nowadays most critical concern. Among the different approaches to convert the heat of low-medium temperature streams into higher quality energy (mechanical or electrical), the employment of energy recovery systems based on an Organic Rankine Cycle (ORC) allows design flexibility with respect to the temperature levels of the application at competitive costs. Furthermore, ORC systems are also suitable to be coupled with renewable energy sources like geothermal, solar and biomass ones. The concept of decentralized electrical energy production fed by renewables is particularly relevant in remote areas and might likely become the cornerstone of a new energy era.

In most of the future ORC applications, target power of the recovery unit will be in the order of few tens of kilowatts. In these systems, operating conditions of the closed loop organic circuit are characterized by small mass flow rates and high pressure rises. Despite large ORC applications (~MW) which could also use centrifugal machines, positive displacement pumps demonstrated to be the most suitable devices for micro-small energy recovery. In particular, volumetric rotary machines outperform reciprocating ones thanks to lower vibrations (i.e. noise), lower pressure and flow pulsations, and a wider capability to match different fluid inlet conditions. Sliding vane types further benefit of geometrical design flexibility that allows to minimize friction losses. Nonetheless, in any small scale pump, performance issues are mainly due to the dimensions that, in turn, lead to lower volumetric and mechanical efficiencies with respect to larger machines.

In the literature, pumping work in ORC systems is hardly discussed due to the direct impact that the expansion machine plays in the actual energy recovery process. In particular, plenty of theoretical works about working fluid selection and optimization of ORC systems are currently available. In these analyses, pump efficiency is assumed as a constant parameter in the calculations regardless of pressure ratio and mass flow rate of the thermodynamic cycle. According to the survey performed in reference [1], pump efficiency values that have been considered range between 65% and 85%. Furthermore, among the conclusions that are stated in these papers, it resulted that specific pumping work decreases for working fluids with high critical temperature (especially if greater than 150°C) while there is not a direct relationship with liquid specific heat [2]. In the experimental works, centrifugal pumps were used in large ORC plants while positive displacement devices, such as diaphragm and scroll types, were employed in medium-small scale systems [1, 3]. However, efficiency is rarely mentioned. In the Authors' opinion, this lack of information might be essentially motivated by the employment of pumps that were not designed for an ORC application even though they were still capable to pressurize the organic working fluids.

In order to remark the relevance of pumping devices for the overall net recovery in an ORC system, the current work presents the development of a sliding vane rotary pump and the assessment of its performances in a low grade energy recovery application for compressed air systems. Experimental data were further used to calibrate a numerical model of the pump which allowed to further explore its capabilities as well as the impact of some design parameters on volumetric and total efficiencies.

2. Experimental activity

The ORC pump presented in this paper is a key device of an innovative power unit for low grade thermal energy recovery applications exclusively based on sliding vane machines. The ORC system displayed in Figure 1 is composed of pump, a sliding-vane rotary expander coupled with an electric generator (whose performances are discussed in reference [4]), and two plate heat exchangers. In particular, the High Temperature Heat Exchanger (HTHE) acts as evaporator while the Low Temperature Heat Exchanger (LTHE) is the condenser of the energy recovery unit. The working fluid was R236fa with the addition of POE lubricant (5% w/w). The hot lube-oil from a sliding vane rotary compressor was used as hot thermal source in HTHE, while the cold source in the LTHE was tap water.

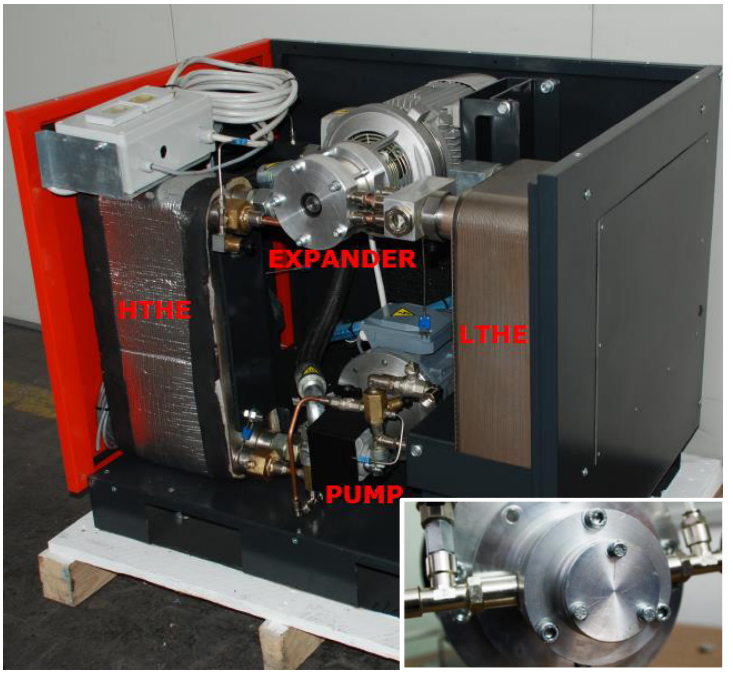

Fig. 1. Energy recovery unit and exterior view of the pump prototype (bottom right)

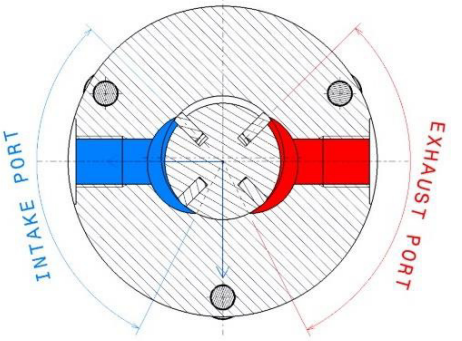

Fig. 2. Cross section view and ports arrangement

Table 1. Design parameters

Rotor diameter	30.0	mm
Stator diameter	32.5	mm
Number of vanes	4	-
Displacement	2	cm^3
Max. operating temperature	120	°C

Pump design was performed not only to maximize its performances but also to achieve a better fitting of the device in the recovery system. The design process led to the geometrical features listed in Table 1. Figure 2 additionally shows a cross section of the machine where intake and exhaust ports are symmetrical and with an angular width of about 90°. The pump was directly coupled with a brushless electric motor that allowed to change the revolution speed of the pump and, in turn, the operating point of the whole recovery system. Furthermore, it additionally provided the direct measurement of revolution speed and the indirect torque measurement from the electrical current. Pressure transducers and T-type thermocouples were also installed across the pump to monitor inlet and outlet thermodynamic conditions of the working fluid. Mass flow rate eventually resulted from the energy balance at the evaporator. Measurements uncertainty is reported in Table 2 and clearly shows that indirect measurement of mass flow rate is highly affected by uncertainty propagation. From a sensitivity analysis, the quantities that mostly contributed to such high uncertainty are the oil temperatures across the evaporator. In a future upgrade of the test bench, a dedicated Coriolis mass flow meter will be installed downstream the pump to allow direct measurements.

Throughout the development stages of the pump, tests were performed using the ORC system as test rig to further appreciate the interactions between each component of the recovery unit such that control strategies could be

outlined. However, the strict link between pump and whole system imposed that fluid pressure rise accomplished by the pump depended on the thermodynamic conditions of the ORC system. The experimental campaign resulted in the operating points listed in Table 2, at different revolution speeds and pressure rises. Inlet conditions were fixed by water temperature at the condenser while outlet absolute pressure could be varied from 8.8 to 12.4 bar. On the other hand, revolution speed ranged from 700 RPM to 1200 RPM. Mass flow rate is proportional to revolution speed and ranged from 52 g/s to 119 g/s while mechanical power, that is related both to mass flow rate and pressure rise, reached up to 289 W.

Table 2. Experimental campaign with measurement uncertainty

test case	1	2	3	4	5	6	7	8	9	
T inlet	24.2	23.6	22.3	20.4	20.2	25.7	18.9	29.5	17.5	± 0.5 °C
T outlet	25.0	24.7	23.2	21.4	21.2	26.5	20.0	30.4	18.8	
p inlet	3.4	3.3	3.3	3.2	3.3	3.7	3.2	3.7	3.1	± 0.1 bar_a
p outlet	12.4	12.1	11.4	10.8	10.6	13.4	9.9	12.4	8.8	
Rev. speed	1200	1100	1000	900	900	1250	800	1300	700	± 1 RPM
Torque	2.3	2.3	2.2	2.1	1.9	2.1	2.0	2.0	2.4	Nm
Mech. power	289	265	230	198	179	275	168	272	176	± 3 W
Mass flow rate	0.110	0.103	0.094	0.086	0.085	0.116	0.071	0.119	0.052	± 9% [kg/s]

3. Numerical model

Past research works on the mathematical modeling of sliding vane machines propose two methodologies: the first and most recent one involves the usage of 3D CFD tools while the latter one is the so-called chamber model. This latter approach models mass and energy exchanges between cells with suction and discharge pipes using a one-dimensional formulation. On the other hand, spatial variation of quantities inside the vanes is collapsed in a lumped parameter approximation whereas equation of state (if the working fluid is a gas) or compressibility relationships (if the working fluid is a liquid) are additionally considered to solve the numerical problem. Due to the high complexity of the computational grid for the fluid domain enclosed between stator, rotor and blades, 3D CFD analyses have been successfully performed on automotive oil pumps, whereas fluid was assumed as incompressible and neglecting any cavitation phenomena [5]. On the other hand, chamber models have been mostly employed on vane machines operating with gases, namely in compressed air [6] and refrigeration applications [7]. The modeling approach pursued in the current research activity is a trade-off between the higher accuracy of 3D CFD and the lower computational cost of chamber models.

The sliding vane pump was modeled in the commercial software GT-SUITE® that is based on a one-dimensional formulation of Navier-Stokes equations and on a staggered grid spatial discretization. According to this approach, any system is discretized into a series of capacities such that manifolds are represented by single volumes while pipes are divided into one or more volumes. These volumes are eventually connected by boundaries. The scalar variables (pressure, temperature, density, internal energy, enthalpy, etc.) are assumed to be uniform over each volume. On the other hand, vector variables (mass flux, velocity, mass fraction fluxes, etc.) are calculated for each boundary [8].

The structure of the ORC pump model displayed in Figure 3.a results from a customization of the GT-SUITE® template for sliding vane machines. In particular, vane pump cells are considered as ducts whose length is the stator one and whose equivalent diameter calculation is based on the instantaneous volume and on inlet and outlet areas of the surfaces that instantaneously face the respective ports. Reference scheme for equivalent diameter calculation is reported in Figure 3.b while its formulation is presented in Eqn. (1).

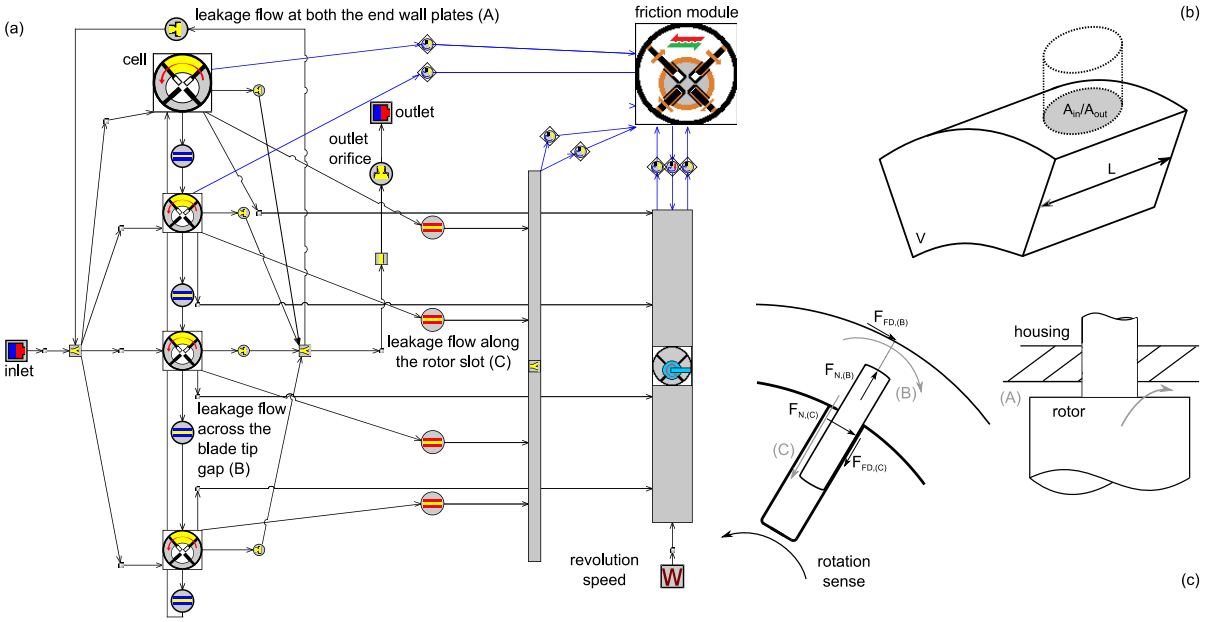

Fig. 3. Numerical model of the sliding vane pump. In GT-SUITE®, the model block diagram (a) considers vanes as equivalent ducts (b) and takes into account three leakage flow paths between vanes and with the housing (c)

The vane machine template accounts for three types of leakage flows: as displayed in Figure 3.c, they may occur between rotor and end wall plates (A), across blades' tips (B) and eventually between vane side and rotor slots (C). In these locations, fluid leaks take place across tight gaps that separate fixed and moving surfaces in relative motion. In turn, in addition to bearings, leakage paths are also sources of viscous friction. Eventually, in locations (B) and (C) dry friction can also occur. While viscous friction was modeled according to the classic definition for Newtonian fluids (Eqn. (2)), dry friction resulted from the calculation of a very simplified blades dynamics (Eqn. (3)).

$$D_{eq} = \max\left(\sqrt{\frac{4V}{\pi L}}, \sqrt{\frac{4A_{in}}{\pi}}, \sqrt{\frac{4A_{out}}{\pi}}\right) \quad (1) \qquad F_{FV} = \mu A \frac{du}{dy} \quad (2) \qquad F_{FD} = f_{dry} F_N \quad (3)$$

In a positive displacement device, it is the flow restriction that the pump sees at its outlet that actually sets the discharge pressure. In the current application, this value was imposed by the hydraulic circuit of the ORC system that included expander, heat exchangers and pipes. Therefore, pressure and temperature measured downstream the pump and listed in Table 2 were set as outlet boundary conditions of the simulations. Same approach was pursued at the inlet boundary environment and for the revolution speed.

One dimensional Navier-Stokes equations were solved with an explicit 5th order Runge-Kutta scheme where primary solution variables are mass flow rate, density, and internal energy. The values of mass flow, density and internal energy at the new time step were eventually calculated through the conservation equations. In order to satisfy the Courant condition that ensures stability to the numerical problem, angular crank angle step was set equal to 1 degree. In turn, actual time step of the simulation depended on crank angle step and revolution speed at the given operating point. In spite of the slightly greater computational cost, the experimental solution scheme allowed to produce more accurate predictions of pressure pulsations.

Model calibration was performed with reference to experimental outlet pressure, mass flow rate and mechanical power. This process would have theoretically required the knowledge of any clearance gaps, dry friction coefficients and their variation with pump operating conditions (pressure rise, temperature, revolution speed). To reduce the

number of simulations, the influence of calibration coefficients on pump performance indicators was identified according to the Design of the Experiment theory [9]. A direct optimization procedure eventually allowed to tune the most relevant calibration coefficients such that numerical results were in agreement with the experimental ones within an error band equal to the measurement uncertainty. Final calibration coefficients are reported in Table 3.

Table 3. Summary of model calibration coefficients

Calibration coefficient	Value
Equivalent diameter of the side leakage path (A in Figure 2.c)	1.41 mm
Clearance between blade tip and stator (B in Figure 2.c)	2 μm
Clearance between rotor slot and blade (C in Figure 2.c)	30 μm
Eccentricity	1.25 mm
Dry friction coefficients (B and C in Figure 2.c)	0.1

Table 4. Friction power decomposition

Moving part	Fixed part	
blade tip	stator	94.0 %
rotor side	end wall plate	0.1 %
blade side	end wall plate	0.1 %
blade side	rotor slot	1.0 %
bearings		4.8 %

Among the simulation outputs, the model provides friction power decomposition and estimates flow rate recirculation across the leakage paths. Friction losses are mainly dominated by power dissipations occurring between stator and tips of the blades, in agreement with more advanced friction models for sliding vane machines [10]. As reported in Table 4, this share exceeds 90% of the total friction losses and does not depend, in relative terms, on revolution speed and pressure rise at which the pump operates. On the other hand, leakages mainly occur between rotor and end wall plates due to the relatively large clearance gap width. Leakages highly depend on pump operating conditions. Hence, their effect could be not summarized as in Table 4 but it was taken into account in the performance map of Figure 6 that is presented in Section 4.

4. Performance maps

The simulation setup retrieved from the calibration process was further employed to assess the pump's capabilities at more extensive regimes such that operating curves and performance maps could be derived. Simulations were performed changing the revolution speed from 1000 RPM to 4000 RPM while outlet pressure of working fluid was varied such that, for the same inlet conditions, pressure rise ranged between 0 and 25 bar. Figure 4 presents the operating points that were simulated and the tendency lines at constant revolution speed. At very low pressure rises (0-5 bar), the operating curves fit a parabolic trend; afterwards the nature of the fit becomes linear, in agreement with the volumetric nature of the sliding vane pump. This behavior reflects experimental observations on a water sliding vane pump where it was additionally shown that operating curves tend to be vertical lines at high revolution speeds due to an improvement of the volumetric efficiency [11]. Indeed, the greater centrifugal force, that occurs at high revolution speeds, lowers the tip clearance gap and, in turn, reduces fluid leakages between consecutive vanes.

The influence of clearance gap between rotor and end wall plates is displayed in Figure 5 with reference to the simulations at 1000 RPM. The chart further reports equations of the tendency curves. If the clearance gap increases, fluid leakages across the most critical location slightly worsen the volumetric efficiency of the pump, as confirmed by the rise of slope in the operating curves.

With reference to Eqns. (4) and (5), performance maps of volumetric and total pump efficiencies were calculated and respectively reported in Figures 6 and 7. Both these figures resulted from a 2D interpolation of the simulations such that the gradient between simulated and interpolated data was as smooth as possible everywhere.

$$\eta_{vol} = \frac{\frac{1}{\rho}\int_{1\,cycle} \dot{m}dt}{N(V_{\max} - V_{\min})} \qquad (4)$$

$$\eta_{tot} = \frac{\dot{m}\Delta p}{\rho \omega T} \qquad (5)$$

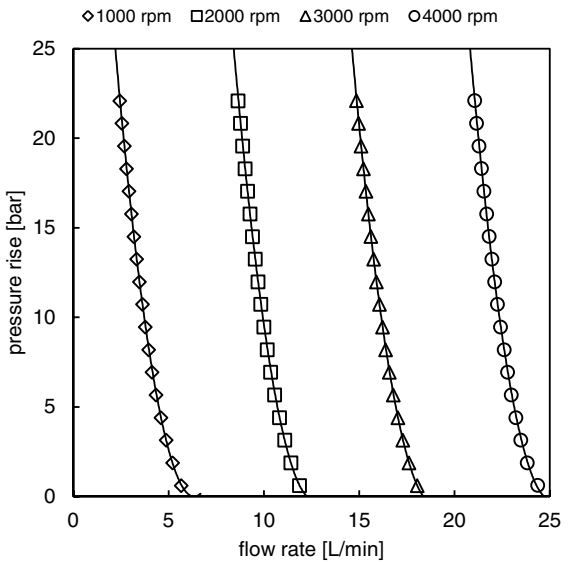

Fig. 4. Operating map

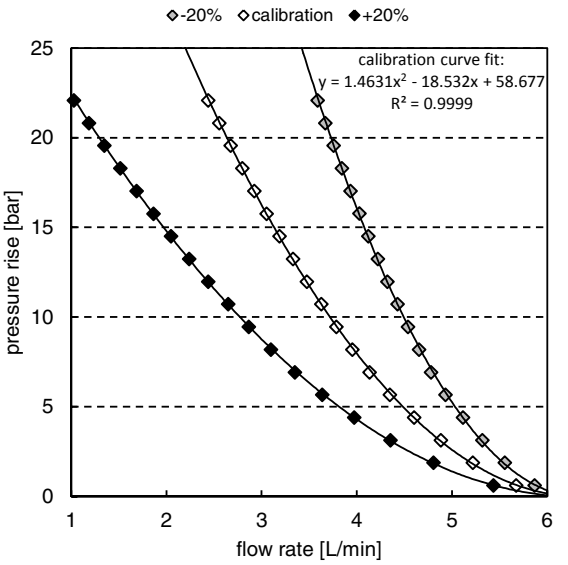

Fig. 5. Effect of side clearance at 1000 RPM

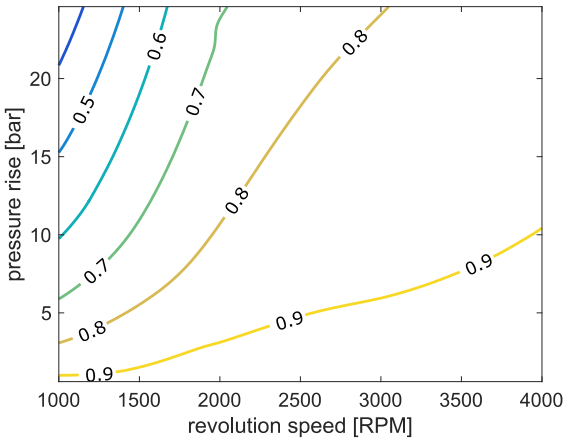

Fig. 6. Volumetric efficiency map

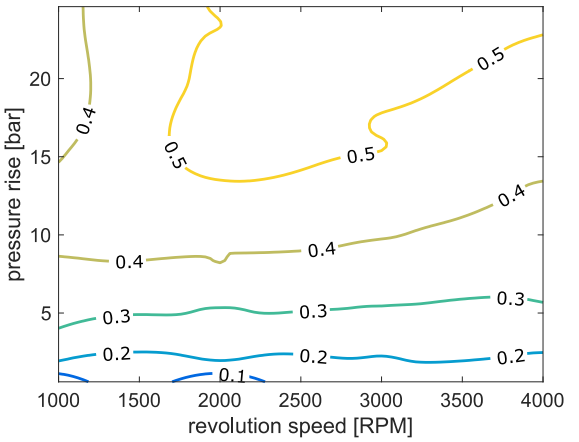

Fig. 7. Total efficiency map

Volumetric efficiency map of Figure 6 shows that in the experimental region (1000-1500 RPM, 0-10 bar) values greater than 85% could be achieved. However, these performances would decrease at high pressure rises since leakage flows are driven by pressure gradients across clearance gaps. On the other hand, higher revolution speeds would lead to significant volumetric efficiency improvements due to the shorter residence time of the leakage flows that would be accounted in a cycle.

Unlike volumetric efficiency that exclusively depends on fluid dynamics, total efficiency additionally accounts for friction phenomena. In particular, the efficiency map reported in Figure 7 shows performances around 20-35% for the experimental region. For a given revolution speed, total efficiency decreases with pressure rise mostly because of worse volumetric performances rather than variations of friction losses. Indeed, the lower amount of fluid that is effectively pressurized by the pump reduces the hydraulic power that is the numerator of Eqn. 5. Although high revolution speeds undoubtedly increase friction losses, this trend is not clearly noticeable in Figure 7 due to the positive action that revolution speed plays on the volumetric features of the pump. This trend was also noticed in

reference [11]. Predicted maximum total pump efficiency should reach 50% at revolution speed higher than 2000 RPM and pressure rises greater than 15 bar.

Since the performance at the state of the art can be mostly attributed to friction, advanced sliding vane pump prototypes will require a proper investigation of diversified design parameters such as geometry and clearances, oil\working fluid mixing ratio and materials. Although the model is not able to relate pump performances to materials, the software platform developed in the current study will be able to support future research by means of parametric analysis to reduce the number of design variables that need to be improved either experimentally or through more advanced numerical investigations.

5. Conclusions

Pumping work in Rankine cycles operating with organic fluids is not negligible as it would be if the working fluid was water. For this reason, an attempt to fill this technological gap has been presented in this research paper through the development of a sliding vane rotary pump specifically conceived to deal with an organic fluid (R236fa). The prototype was tested on an innovative small-scale energy recovery unit which is suitable for low-medium temperature waste heat streams. In the current study, the ORC unit was coupled to a high-efficiency sliding vane air compressor: hot source was the compressor's lubricant while the cold one was tap water. Revolution speed and outlet pressure were the parameters which could be varied such that cycle pressure ratios between 2.8 and 3.7 and mass flow rates between 0.05 kg/s and 0.12 kg/s could be provided by the sliding vane pump. In these experimental conditions, the mechanical power input ranged between 170 W and 390 W. The experimental campaign was further taken as reference to calibrate a one-dimensional model of the pump that allowed to outline performance maps of the pump in a more extensive operating range. In particular, the pump shows very attractive values for volumetric efficiencies while total efficiency still needs to be improved in order to exceed the current values that are around 35%. The model additionally provided a decomposition of the overall power losses due to friction showing that the most relevant location is the region between stator and blade tip. On the other hand, the major source of leakages is the gap between rotor and end wall plates. The know-how acquired through these experimental and modeling activities will be the baseline for the development of advanced sliding vane ORC pump prototypes that are going to be tested on a dedicated test bench to achieve a greater operational flexibility and a better measurement accuracy.

References

[1] Aleksandra Borsukiewicz-Gozdur, Pumping work in the organic Rankine cycle, Applied Thermal Engineering, Volume 51, Issues 1–2, March 2013, Pages 781-786, ISSN 1359-4311, DOI:10.1016/j.applthermaleng.2012.10.033.

[2] J. Bao and L. Zhao, A review of working fluid and expander selections for organic Rankine cycle, Renewable and Sustainable Energy Reviews, Volume 24, August 2013, Pages 325-342, ISSN 1364-0321, DOI:10.1016/j.rser.2013.03.040.

[3] J. Lopes et al., Review of Rankine cycle systems components for hybrid engines waste heat recovery, SAE Technical Paper 01 (1942). DOI:10.4271/2012-01-1942.

[4] R. Cipollone et al., Mechanical Energy Recovery from Low Grade Thermal Energy Sources, Proceedings of the 68th Conference of the Italian Thermal Machines Engineering Association, Energy Procedia, Volume 45, 2014, Pages 121-130, ISSN 1876-6102, DOI: 10.1016/j.egypro.2014.01.014

[5] Q.Zhang and X. Y. Xu, Numerical Simulation on Cavitation in a Vane Pump with Moving Mesh, 5th International Conference on Computational Methods, 28-30th July 2014, Cambridge, England

[6] G. Bianchi and R. Cipollone, Theoretical modeling and experimental investigations for the improvement of the mechanical efficiency in sliding vane rotary compressors, Applied Energy, Volume 142, 15 March 2015, Pages 95-107, ISSN 0306-2619, DOI: 10.1016/j.apenergy.2014.12.055

[7] Osama Al-Hawaj, Theoretical modeling of sliding vane compressor with leakage, International Journal of Refrigeration, Volume 32, Issue 7, November 2009, Pages 1555-1562, ISSN 0140-7007, DOI:10.1016/j.ijrefrig.2009.07.005.

[8] Gamma Technologies, Flow theory manual, GT-Suite Version 7.5.

[9] D. C. Montgomery, Design and analysis of experiments, John Wiley & Sons, 2008.

[10] G. Bianchi and R. Cipollone, Friction power modeling and measurements in sliding vane rotary compressors, Applied Thermal Engineering, Volume 84, 5 June 2015, Pages 276-285, ISSN 1359-4311, DOI: 10.1016/j.applthermaleng.2015.01.080

[11] R. Cipollone et al., Fuel economy benefits of a new engine cooling pump based on sliding vane technology with variable eccentricity, Energy Procedia, Volume 82, 2015, Pages 265-272, ISSN 1876-6102, DOI: 10.1016/j.egypro.2015.12.032